Confounded spikes generated by synchrony within neural tissue models

Kenneth P. Eaton [a,*], Craig S. Henriquez [a]

[a] *Center for Neuroengineering and Department of Biomedical Engineering, Duke University, Durham, NC*

Abstract

Spike-sorting often requires subjective interpretation of the waveforms to resolve the underlying neural activity. Often, multiple waveforms are detected at one site and interpreted as arising from multiple neurons. Because uncovering the relationship between the spike and the underlying intracellular activity is not tractable in vivo, a computer model of 128 multi-compartment neurons sharing common inputs was used to explore how synchronous firing impacts both the morphology and classification of the spikes. The results suggest that near-synchronous conditions yield multiple waveforms that could lead to missed spikes and a confounded interpretation of the number of neurons contributing to the recording.

Key words: Confounded spikes, Neural synchrony, Spike detection

* Corresponding author.
Email addresses: kpe@duke.edu (Kenneth P. Eaton), ch@frosty.mc.duke.edu (Craig S. Henriquez).

1 Introduction

Efficient extraction of single-unit activity from extracellular recordings is a critical step toward understanding the signaling in a population of neurons. The extraction and classification process, however, is often subjective due to spike-to-spike variations in the action potentials of single neurons (such as would occur during burst activity) and the fact that the activity from multiple neurons can be detected at a single site. Simultaneous intracellular-extracellular recording has been used to verify the reliability of spike separation methods [3] as well as to investigate how intracellular changes lead to variation in the measured extracellular spike [4]. A limitation of this technique is that only one neuron can be recorded intracellularly, so only one extracellular waveform can be verified. An alternative approach is to use computer simulation where multiple factors involved in the generation of the extracellular signal can be controlled and varied. In this study, a computer model of densely-packed, realistic multi-compartment neurons was used to determine how the synchronous firing of adjacent neurons impact both the the morphology and classification of the detected spikes. The results suggest that near-synchronous conditions yield a wide variety of distinct waveforms that could lead to missed spikes and a confounded interpretation of the number of cells contributing to a recording.

2 Methods

The model used for generating the extracellular waveforms was comprised of 128 densely-packed thalamic reticular neurons (Fig. 1). This dendritic model

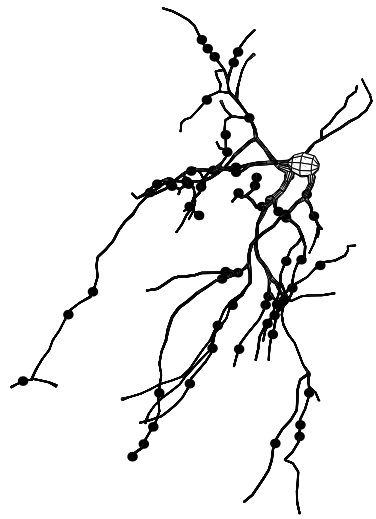

Fig. 1. Dendritic structure of the thalamic reticular neuron adapted from [1], comprised of 424 compartments. Black circles indicate the positions of 64 AMPA synapses [2]. Each of these synapses had a maximum conductance of 1 nS and was driven with an independent, Poisson-random input with an average firing rate of 20 Hz, a 1 msec activation time, and a 2 msec refractory period.

was adapted from data taken from Destexhe et al. [1]. All parameter values (i.e. ion channel conductances) were the same as those used in [1] with the exception of the axial resistivity. This was reported as 260±30 Ωcm, so each of the 128 neurons was given a random axial resistivity within this range. Each neuron had 64 AMPA synapses [2] randomly positioned along its dendrites (Fig. 1, black circles). The 128 neurons were laid out in stacked layers as shown in Fig. 2A. The extracellular potential at any site in the tissue was computed using a monopolar source model such that every compartment was treated as a point source of current (equivalent method of [5]). A site near the center of the population of neurons was chosen to compute the extracellular potential. This site was located closest to two neurons indicated in Fig. 2A by circled points. An expanded view of the network is shown in Fig. 2B. The simulated recording site (gray sphere) was located nearest to the cell body of the lower neuron (R1) and inside the dendritic arbor of the upper neuron (R2). The average extracellular waveform measured during a spike from R1 is shown in Fig. 2C. Because only the cell body was capable of initiating

action potentials, it acted as a current sink relative to its dendrites and the extracellular potential nearby had an initial negative deflection. By contrast, the extracellular spike from R2 had an initial positive deflection when R2 fired (Fig. 2D) since the dendrites acted as current sources.

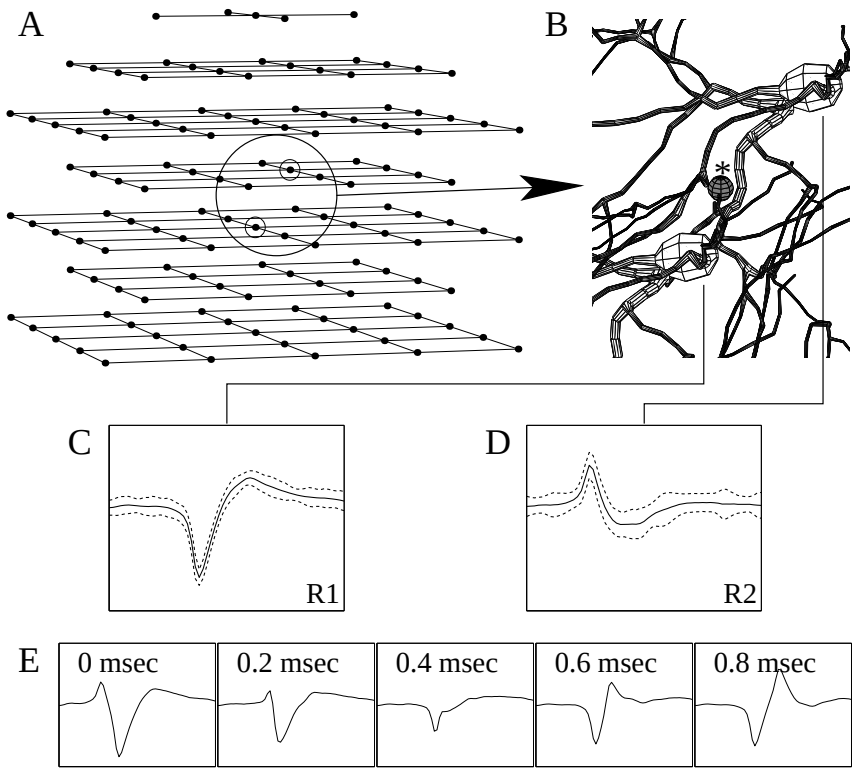

Fig. 2. **A:** Within each layer of the network neurons were separated by 100 μm in both directions. Layers were separated by 50 μm and were alternating 5-by-5 and 4-by-4 grids. **B:** Expanded view of the network in the region surrounding the simulated recording site (gray sphere with asterisk above it). **C:** Average extracellular trace from neuron R1. **D:** Average extracellular trace from neuron R2. **E:** Confounded waveforms generated by adding delayed versions of D to C (delay indicated on graph). Window sizes are 3 msec by 80 μV.

Given the relative locations of the cell bodies and the recording site, R1 and R2 were the only neurons with extracellular spikes of sufficient amplitude to be recognized. The other 126 neurons therefore acted primarily as background

current sources during the simulation. Since R1 and R2 shared no direct connections, various levels of synchrony were established by inputing the same Poisson-random signals into some fraction of their synapses, thereby creating a set of synaptic inputs common to both neurons. Possible results of this enhanced synchrony are shown in Fig. 2E where the waveforms of R1 and R2 are added with different time offsets to create a variety of confounded waveforms. Three simulations were run with three percentages of common synaptic inputs: 0% (independent), 95% (61 of 64 synapses common), and 100% (all synapses common). In each case, the intracellular voltages for R1 and R2 and the generated extracellular potential were recorded. The extracellular waveforms were then analyzed with Plexon Offline Sorter (OFS) software.

3 Results

The results of the simulation with 0% common inputs are shown in Fig. 3. The raster plot shows, from top to bottom, the two actual spike trains for R1 (black) and R2 (light gray) found using the intracellular voltage waveforms, the units S1–S4 (gray) found with the spike-sorter, and the spikes that were missed for R1 (M1, black) and R2 (M2, light gray). A missed spike was designated as a spike for R1 or R2 that had no corresponding spike in S1–S4 within a window of ±600 msec. For R1, R2, M1, and M2 the total numbers of spikes are shown on the right. For S1–S4 the numbers on the right are the numbers of spikes in that unit that correlate with a spike from R1 and R2, respectively. A unit spike was said to correlate with a spike from R1 or R2 if that spike fell within a window of ±600 msec of the unit spike. The graphs at the left show the average unit waveforms. As Fig. 3 shows, S1 correlates strongly with R1

and S2 correlates strongly with R2. Confounded units (S3 and S4) occur with a relatively low frequency and do not have a distinct waveform, as expected from the lack of common inputs. More spikes are missed from R2 than from R1 due to its lower amplitude.

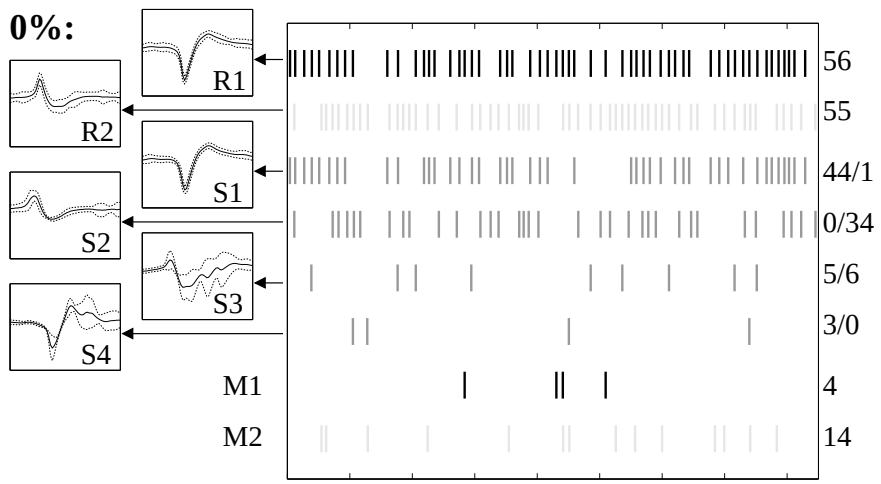

Fig. 3. Results for 0% common input simulation. Average unit waveforms are shown on the left. For R1, R2, M1, and M2, the total number of spikes are shown on the right. For S1–S4, the numbers on the right are the numbers of spikes in that unit that correlate with a spike in R1 and R2, respectively.

Fig. 4 shows the results for the 95% (top) and 100% (bottom) common input simulations. In the 95% case, the waveforms for S1 and S2 still closely match those of R1 and R2, but the number of spikes that correlate between them are reduced (30 between S1 and R1 and 26 between S2 and R2). There are more spikes attributed to confounded units, and unit S4 in particular has a more distinct waveform. Comparing the raster plots of S4 and M2, there is a strong correlation between the detection of a spike for S4 and a missed spike detection for R2. Inspecting the unit waveform of S4 shows that it corresponds to a firing of R1 with a late firing of R2. The R2 spike is often undetected as a result, but it creates a new waveform with a wider, double-humped second peak. In the extreme 100% common input case, R1 and R2 are *nearly* synchronized but

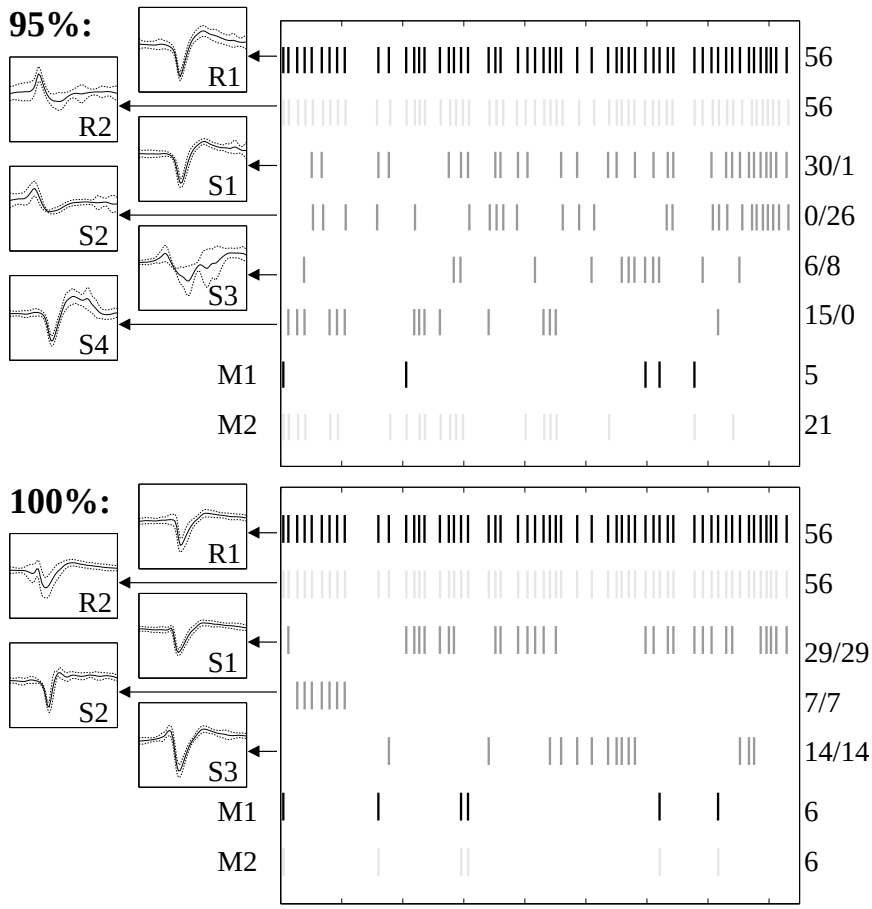

Fig. 4. Results for 95% and 100% common input simulations. Average unit waveforms are shown on the left. For R1, R2, M1, and M2, the total number of spikes are shown on the right. For S1–S4, the numbers on the right are the numbers of spikes in that unit that correlate with a spike in R1 and R2, respectively.

not *perfectly* synchronized due to the assigned variation in the axial resistivity between neurons. One effect of the synchrony is that the R2 waveform cannot be reliably detected even using the intracellular voltage trace. R1 shows some variation as well. Unit S1 resembles R1, but S2 has a narrower peak and S3 has a slightly larger amplitude and appears more triphasic. The raster plots of S1–S3 suggest that instead of having two synchronously-firing units, there are three units that fire in distinct, exclusive bursts.

4 Conclusions

The simulation studies showed that extracellular measurements taken in regions where there is likely to be strong synchrony of firing between two or more neurons will produce a larger number of confounded units, suggesting that more neurons are contributing to the signal than are actually present. In real tissue, neurons would not only share some percentage of common inputs but also have direct connections to one another (or connections through interneurons). Additionally, field effects have been shown to further enhance synchrony in regions such as hippocampal CA1 [6,7]. Hence, the likelihood of closely spaced neurons firing synchronously and generating confounded spikes is high. Investigating the effect of synchrony on spike-sorting techniques would be a difficult task in vivo because of the need to make intracellular recordings from a number of closely spaced neurons. By using detailed computer models of neural tissue, the effects of synchronous firing can studied in detail since all potentials and currents are available. The consequence of using these confounded spikes in some analysis method, however, is unclear and likely problem dependent. But the fact that spikes from two cells may be misinterpreted as arising from multiple cells will produce a different picture of underlying neural activity than what actually exists. As as result, new electrode designs or analysis techniques will need to be developed to compensate for the presence of confounded spikes in the recorded signal due to various levels of synchrony in clusters of neurons.

Acknowledgements

Thanks to Rui Costa for spike-sorting and helpful discussions. This work was supported by DARPA grant DARPA-SPAWAR N66001-02-C-8022 and NSF grant NSF-IBN-99-80043.

References

[1] A. Destexhe, D. Contreras, M. Steriade, T. J. Sejnowski, and J. R. Huguenard, In vivo, in vitro, and computational analysis of dendritic calcium currents in thalamic reticular neurons, *J. Neurosci.* **16** (1996) 169–185.

[2] A. Destexhe, Z. F. Mainen, and T. J. Sejnowski, Kinetic models of synaptic transmission, in: C. Koch and I. Segev (Eds.), Methods in Neuronal Modeling, 2nd Edition, MIT Press, Cambridge, MA, 1998, pp. 1–25.

[3] K. D. Harris, D. A. Henze, J. Csicsvari, H. Hirase, and G. Buzsáki, Accuracy of Tetrode Spike Separation as Determined by Simultaneous Intracellular and Extracellular Measurements, *J. Neurophysiol.* **84** (2000) 401–414.

[4] D. A. Henze, Z. Borhegyi, J. Csicsvari, A. Mamiya, K. D. Harris, and G. Buzsáki, Intracellular Features Predicted by Extracellular Recordings in the Hippocampus In Vivo, *J. Neurophysiol.* **84** (2000) 390–400.

[5] K. M. L. Menne, A. Folkers, T. Malina, R. Maex, and U. G. Hofmann, Test of spike-sorting algorithms on the basis of simulated network data, *Neurocomputing* **44–46** (2002) 1119–1126.

[6] C. P. Taylor and F. E. Dudek, Synchronization Without Active Chemical Synapses During Hippocampal Afterdischarges, *J. Neurophysiol.* **52** (1984) 143–155.

[7] R. D. Traub, F. E. Dudek, C. P. Taylor, and W. D. Knowles, Simulation of Hippocampal Afterdischarges Synchronized by Electrical Interactions, *Neurosci.* **14** (1985) 1033–1038.

Kenneth Eaton received the B.S. degree in biomedical engineering from Boston University in 1999. Since then, he has been working toward his Ph.D. in computational neural electrophysiology at Duke University. His research focuses on using complex large-scale models of neural interactions to study aspects of the generation of extracellular potentials within neural tissue.

Craig Henriquez received the B.S.E. degree in biomedical and electrical engineering from Duke University, Durham, NC, in 1981. After teaching high school for two years, he returned to Duke and received the Ph.D. degree in biomedical engineering in 1988. He became a Research Assistant Professor in 1989 and an Assistant Professor of Biomedical Engineering in 1991 at Duke University. He is currently the W. H. Gardner, Jr. Associate Professor of Biomedical Engineering and Computer Science at Duke University. He is also the Co-Director of Duke's Center for Neuroengineering. His research interests include cardiac and neural electrophysiology, large-scale computer modeling, and neural analysis.